Broadband large-ellipticity harmonic generation with polar molecules

Meiyan Qin[1],Xiaosong Zhu[1], Qingbin Zhang[1], Weiyi Hong[1†], and Peixiang Lu[1,2]

[1] *Wuhan National Laboratory for Optoelectronics and School of Physics, Huazhong University of Science and Technology, Wuhan 430074, P. R. China*

[2] *Laboratory of Optical Information Technology, Wuhan Institute of Technology, Wuhan 430073, P. R. China*

*hongweiyi@mail.hust.edu.cn

Abstract: We investigate the polarization properties of high harmonic generation from polar molecules with a linearly polarized field. It is found that elliptically polarized harmonics are observed in a wide spectral range from the plateau to the cutoff. Further analyses show that the nonsymmetric structure of the highest occupied molecular orbital is the origin of ellipticity of the harmonics. The results provide a method for generation of large-ellipticity XUV pulses, which will benefit the application of HHG as a tool of detection in materials and biology science.

OCIS codes: (190.7110) Ultrafast nonlinear optics; (190.4160) Multi-harmonic generation; (300.6560) Spectroscope, x-ray

References and links

1. F. Krausz, "Attosecond physics," Rev. Mod. Phys. **81,** 163-234(2009).
2. P. Lan, P. Lu, W. Cao, Y. Li, and X. Wang, "Isolated sub-100-as pulse generation via controlling electron dynamics," Phys. Rev. A **76,** 011402(R) (2007).
3. W. Cao, P. Lu, P. Lan, X. Wang, and Y. Li, "Control of the launch of attosecond pulses," Phys. Rev. A **75,** 063423 (2007).
4. P. Lan, P. Lu, F. Li, Y. Li, and Z. Yang, "Carrier-envelope phase measurement from half-cycle high harmonics," Opt. Express **16,** 5868-5873 (2008).
5. W. Cao, P. Lu, P. Lan, X. Wang, and G. Yang, "Single-attosecond pulse generation with an intense multicycle driving pulse ," Phys. Rev. A **74,** 063821 (2006).
6. J. Itatani, J. Levesque, D. Zeidler, Hiromichi Niikura, H.Pépin, J. C. Kieffer, P. B. Corkum, and D. M. Villeneuve, "Tomographic imaging of molecular orbitals," Nature **432,** 867(2004).
7. Manfred Lein, "Molecular imaging using recolliding electrons," J. Phys. B: At. Mol. Opt. Phys **40,** R135-R173 (2007).
8. M. Lein, N. Hay, R. Velotta, J. P. Marangos, and P. L. Knight, "Role of the intramolecular phase in high-harmonic generation," Phys. Rev. Lett **88,** 183903 (2002).
9. W. Hong, P. Lu, Q. Li, and Q. Zhang, "Broadband water window supercontinuum generation with a tailored mid-IR pulse in neutral media," Opt. Lett. **34,** 2102-2104 (2009).
10. Z. Chang, "Single attosecond pulse and xuv supercontinuum in the high-order harmonic plateau," Phys. Rev. A **70,** 043802 (2004).
11. W. Hong, P. Lu, P. Lan, Q. Zhang, and X. Wang, "Few-cycle attosecond pulses with stabilized-carrier-envelope phase in the presence of a strong terahertz field ," Opt. Express **17,** 5139-5146 (2009).
12. E. Hijano, C. Serrat, G. N. Gibson, and J. Biegert, "Orbital geometry determined by orthogonal high-order harmonic polarization components," Phys. Rev. A **81,** 041401(R) (2010).
13. J. Levesque, Y. Mairesse, N. Dudovich, H. Pépin, J. C. Kieffer, P. B. Corkum, and D. M. Villeneuve, "Polarization state of high-order harmonic emission from aligned molecules," Phys. Rev. Lett **99,** 243001 (2007).
14. S. Ramakrishna, Paul A. J. Sherratt, A. D. Dutoi, and T. Seideman, "Origin and implication of ellipticityin high-order harmonic generation from aligned molecules," Phys. Rev. A **81,** 021802(R) (2010).

15. Y. Mairesse, J. Higuet, N. Dudovich, D. Shafir, B. Fabre, E. Mével, E. Constant,S. Patchkovskii, Z. Walters, M. Yu. Ivanov, and O. Smirnova, "Hihg harmonic spectroscopy of multichannel dynamics in strong-field ionization," Phys. Rev. Lett **104,** 213601 (2010).
16. O. Smirnova, S. Patchkovskii, Y. Mairesse, N. Dudovich, D. Villeneuve, P. Corkum, and Misha Yu.Ivanov, "Attosecond circular dichroism spectroscopy of polyatomic molecules," Phys. Rev. Lett **102,** 063601 (2009).
17. V. V. Strelkov, A. A. Gonoskov, I. A. Gonoskov, and M. Yu. Ryabikin, "Origin for ellipticity of high-order harmonics generated in atomic gases and the sublaser-cycle evolution of harmonic polarization," Phys. Rev. Lett **107,** 043902(2011).
18. Q. Zhang, P. Lu, P. Lan, W. Hong, and Z. Yang, "Multi-cycle laser-driven broadband supercontinuum with a modulated polarization gating , " Opt. Express **16,** 9795-9803 (2008).
19. Xibin Zhou, Robynne Lock, Nick Wagner, Wen Li, Henry C. Kapteyn, and Margaret M. Murnane, "Elliptically polarized high-order harmonic emission from molecules in linearly polarized laser fields," Phys. Rev. Lett **102,** 073902 (2009).
20. A. Etches, C. B. Madsen, and L. B. Madsen, "Inducing elliptically polarized high-order harmonics from aligned molecules with linearly polarized femtosecond pulses," Phys. Rev. A **81,** 013409 (2010).
21. Sang-Kil Son, D. A. Telnov, and Shih-I Chu, "Probing the origin of elliptical high-order harmonic generation from aligned molecules in linearly polarized laser fields," Phys. Rev. A. **82,** 043829 (2010).
22. Anh-Thu Le, R. R. Lucchese, and C. D. Lin, "Polarization and ellipticity of high-order harmonics from aligned molecules generated by linearly polarized intense laser pulses," Phys. Rev. A **82,** 023814 (2010).
23. P. A. Sherratt, S. Ramakrishna, and T. Seideman, "Signatures of the molecular potential in the ellipticity of high-order harmonics from aligned molecules," Phys. Rev. A **83,** 053425(R) (2011).
24. M. Lewenstein, Ph. Balcou, M. Yu. Ivanov, A. L'Huillier, and P. Corkum, "Theory of high-harmonic generation by low-frequency laser fields," Phys. Rev. A **49,** 2117-2132 (1994).
25. S. Ramakrishna, and T. Seideman, "Information content of high harmonics generated from aligned molecules," Phys. Rev. Lett **99,** 113901 (2007).
26. P. Lan, P. Lu, Q. Li, F. Li, W. Hong, and Q. Zhang, "Macroscopic effects for quantum control of broadband isolated attosecond pulse generation with a two-color field," Phys. Rev. A **79,** 043413 (2009).
27. W. Hong, P. Wei, Q. Zhang, S. Wang, and P. Lu, "Mid-infrared modulated polarization gating for ultra-broadband supercontinuum generation," Opt. Express **18,** 11308-11315 (2010).
28. X. M. Tong, Z. X. Zhao, and C. D. Lin, "Theory of molecular tunneling ionization," Phys. Rev. A **66,** 033402(2002).Opt. Express **16,** 9795-9803 (2008).
29. M. J. Frisch, G. W. Trucks, H. B. Schlegel, G. E. Scuseria, M. A. Robb, J. R. Cheeseman, J. A. Montgomery Jr., T. Vreven, K. N. Kudin, J. C. Burant, J. M. Millam, S. S. Iyengar, J. Tomasi, V. Barone, B. Mennucci, M. Cossi, G. Scalmani, N. Rega, G. A. Petersson, H. Nakatsuji,M. Hada,M. Ehara, K. Toyota, R. Fukuda, J. Hasegawa,M. Ishida, T. Nakajima, Y. Honda, O. Kitao, H. Nakai, M. Klene, X. Li, J. E. Knox, H. P. Hratchian, J. B. Cross, V. Bakken, C. Adamo, J. Jaramillo, R. Gomperts, R. E. Stratmann, O. Yazyev, A. J. Austin, R. Cammi, C. Pomelli, J. W. Ochterski, P. Y. Ayala, K. Morokuma, G. A. Voth, P. Salvador, J. J. Dannenberg, V. G. Zakrzewski, S. Dapprich, A. D. Daniels, M. C. Strain, O. Farkas, D. K. Malick, A. D. Rabuck, K. Raghavachari, J. B. Foresman, J. V. Ortiz, Q. Cui, A. G. Baboul, S. Clifford, J. Cioslowski, B. B. Stefanov, G. Liu, A. Liashenko, P. Piskorz, I. Komaromi, R. L. Martin, D. J. Fox, T. Keith, M. A. Al-Laham, C. Y. Peng, A. Nanayakkara, M. Challacombe, P. M. W. Gill, B. Johnson, W. Chen, M. W. Wong, C. Gonzalez, and J. A. Pople, Gaussian 03, Revision C.02, Gaussian Inc., Wallingford, CT (2010).
30. Z. Zhao, J. Yuan, and T. Brabec, "Multielectron signatures in the polarization of high-order harmonic radiation," Phys. Rev. A. **76,** 031404(R) (2007)
31. P. B. Corkum, "Plasma perspective on strong field multiphoton ionization," Phys. Rev. Lett **71,** 1994-1997 (1993).

1. Introduction

High harmonic generation (HHG) has attracted significant attention for producing coherent attosecond pulses in the XUV regime [1–5] and detecting the molecular structure as well as attosecond electronic dynamics [6–8]. The power spectrum of high harmonic emission has been extensively studied in previous experimental and theoretical investigations [9–11]. Recently, the polarization characteristics of the harmonic emission are also actively studied due to the potential applications of elliptically polarized harmonics. It is found that information about the molecular system participating in the harmonic generation can be imprinted in the polarization characteristics of harmonics [12–14]. Therefore elliptically polarized harmonics can provide a sensitive probe of the molecular system. For example, Y. Mairesse *et al.* [15] both theoretically and experimentally demonstrated that elliptically polarized harmonics can be applied in HHG spectroscopy of oriented N_2 to track multichannel dynamics during strong-field ionization. In

addition, the search for ellipticity in HHG is also motivated by the generation of elliptically (even circularly) polarized attosecond pulses in the xuv regime [16].

Several attempts have been made to obtain large ellipticity in the harmonics. It has been shown that the nonlinearly polarized harmonics can be obtained using an elliptically polarized driving laser [17]. In such case, the harmonic efficiency drops significantly with increasing ellipticity of the driving laser [18]. The elliptically polarized harmonics are also observed when the oriented molecule is driven by a linearly polarized laser [19–23]. Previous works have proposed several origins of the nonzero ellipticity of the harmonics generated from oriented molecules. For example, both two-center [20, 21] and channel [16] interference, which can result in structural and dynamical minima respectively, are responsible for the elliptically polarized harmonics. In detail, the structural and dynamical minima in the parallel component of the harmonics make the amplitude of the parallel and perpendicular components comparable. Meanwhile, a phase jump by $\sim \pi$ of the parallel component is accompanied by the interference minimum position, leading to the phase difference between the two components passing through $\pi/2$. Therefore the harmonics in the vicinity of the interference minima are elliptically polarized. Recently, Ramakrishna *et al.* [14] demonstrated that the molecular potential also plays an important role in determining the polarization properties of the harmonics. In previous investigations, the targets are either atoms or non-polar molecules such as H_2, CO_2, O_2, and N_2. However, the polarization characteristics of the harmonics generated from polar molecules are seldom studied to the best of our knowledge. The orbital symmetry is one of the basic properties of molecules and can embody the difference between the polar and non-polar molecules. Nonetheless, its influence on the elliptical polarization is also seldom investigated.

In this paper, we investigate the polarization characteristics of HHG from the polar molecules with a linearly polarized laser and analyze the influence of the structure of the highest occupied molecular orbital (HOMO). Our results show that for oriented polar molecules strongly elliptically polarized harmonics are observed in a spectral range from the plateau to the cutoff at the orientation angles ranging from 30° to 80°. Further analyses reveal that the nonsymmetric structure of the HOMO is responsible for those polarization characteristics of the harmonics in the case of oriented polar molecules.

2. Theoretical model

In this paper, we use the example of CO to investigate the polarization characteristics of the harmonic emission from oriented polar molecules driven by a linearly polarized laser. Our coordinate system, depicted in Fig. 1(a), defines the polarization vector of the driving pulse as the space-fixed **z** axis, with the molecular axis **z1** lying in the y-z plane. The orientation angle between the molecular axis (**z1**) and the driving laser polarization axis (**z**) is denoted as θ. Note that we only need to consider the **y**, **z** components of the harmonic emission, since the **x** component along the propagation direction of the driving laser cannot be phase matched [19, 22]. In Fig. 1(b), an illustration of the HHG ellipse is presented. The major, minor axes of the ellipse are denoted as **a**, **b** respectively. ϕ represents the rotation angle of the major axis (**a**) of the HHG ellipse with respect to the polarization axis (**z**) of the driving laser field. Ellipticity of HHG ε is defined as the ratio of the length between the minor and major axes, i.e. $\varepsilon = b/a$.

The simulations are carried out using the extended strong field approximation (SFA) model [24]. With its analytical and fully quantum-mechanical formulations for harmonics, one can explicitly and directly analyze the influence of the orbital symmetry of the HOMO. In present work, the main focus is the ellipticity of the harmonics, which is dominantly influenced by the electronic dynamics. The rotational dynamics are not taken into account by assuming a perfect orientation, which is analogous to [20, 21]. More sophisticated theory that takes both the rotations and the molecular potential into account is presented in recent works [14, 23, 25].

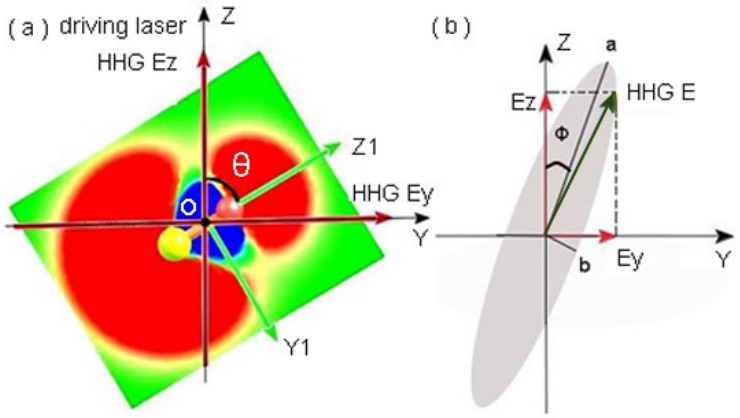

Fig. 1. (Color online) (a) An illustration of the laboratory coordinate system. (**x**,**y**,**z**) is the laboratory frame,the driving laser field propagates along the **x** axis and oscillates along the **z** axis. The orientation angle θ is positive for clockwise rotation from the **z** direction. (b) An illustration of HHG ellipse. The **a**, **b** axes are the major, minor axes of the ellipse respectively. ϕ is the rotation angle of the **a** axis with respect to the **z** axis.

Within the SFA model, the **y**, **z** components of the laser-induced dipole moments responsible for harmonic emission are expressed as (in atomic units)

$$\begin{aligned} r_y(t;\theta) &= i\int_{-\infty}^{t} dt' \left[\frac{\pi}{\zeta + i(t-t')/2}\right]^{3/2} E(t')g(t';\theta)d_z\left[p_{st}(t',t)+A(t');\theta\right] \\ &\quad \times exp\left[-iS_{st}(t',t)\right] g^*(t;\theta)d_y^*\left[p_{st}(t',t)+A(t);\theta\right] + c.c.. \end{aligned} \tag{1}$$

$$\begin{aligned} r_z(t;\theta) &= i\int_{-\infty}^{t} dt' \left[\frac{\pi}{\zeta + i(t-t')/2}\right]^{3/2} E(t')g(t';\theta)d_z\left[p_{st}(t',t)+A(t');\theta\right] \\ &\quad \times exp\left[-iS_{st}(t',t)\right] g^*(t;\theta)d_z^*\left[p_{st}(t',t)+A(t);\theta\right] + c.c.. \end{aligned} \tag{2}$$

In these equations, $E(t)$ refers to the electric field of the driving laser pulse, $A(t)$ is its associated vector potential, ζ is a positive constant, t' and t correspond to the moments of electronic ionization and recombination respectively, p_{st} and S_{st} are the stationary momentum and the quasi-classical action, which are given by

$$p_{st}(t',t) = \frac{1}{t-t'}\int_{t'}^{t} A(t'')dt'', \tag{3}$$

$$S_{st}(t',t) = (t-t')I_p - \frac{1}{2}p_{st}^2(t',t)(t-t') + \frac{1}{2}\int_{t'}^{t} A^2(t'')dt'', \tag{4}$$

where I_p is the ionization energy of the target molecule. $g(t;\theta)$ represents the ground state amplitude at the time t, and can be expressed as [26,27]:

$$g(t;\theta) = exp\left[-\int_{-\infty}^{t} w(t';\theta)dt'\right]. \tag{5}$$

$w(t';\theta)$ is the ionization rate, which is calculated by Molecular Ammosov-Delone-Krainov (MO-ADK) model for aligned molecules [28]. $\vec{d}(p)$ is the field-free dipole matrix element for

transition from the ground state to the continuum state, where p stands for the momentum of the electron. d_y, d_z correspond to its **y**, **z** components, respectively. Within the single active electron approximation (SAE), this transition dipole moment is given by [13]

$$\vec{d}(p;\theta) = \langle \psi_0(x,y,z;\theta)|\vec{r}|\psi_p\rangle. \tag{6}$$

Here $\psi_0(x,y,z;\theta)$ represents the ground state of the target molecule, i.e. the highest occupied molecular orbital (HOMO). The HOMO is obtained using the Gaussian 03 ab initio code [29] with the 3-21G basis set. $\psi_p = \exp(ipz)$ refers to the electronic continuum state with a momentum p. The harmonic spectrum is then obtained by Fourier transforming the time-dependent dipole acceleration $\vec{a}(t;\theta)$. The equations for the two components are:

$$a_y(q;\theta) = \frac{1}{T}\int_0^T a_y(t;\theta)exp(-iq\omega t)dt, \tag{7}$$

$$a_z(q;\theta) = \frac{1}{T}\int_0^T a_z(t;\theta)exp(-iq\omega t)dt, \tag{8}$$

where $\vec{a}(t;\theta) = \ddot{\vec{r}}(t;\theta)$, T and ω are the duration and frequency of the driving pulse, q corresponds to the harmonic order. The spectral intensity (I) and phase (φ) of harmonic components are given by $I_j(q) = |a_j(q)|^2$, $\varphi_j(q) = \arg[a_j(q)]$, $j = y,z$. The ellipticity ε is determined by the amplitude ratio and the phase difference of the two components [21]:

$$\varepsilon = \sqrt{\frac{1+r^2-\sqrt{1+2r^2\cos 2\delta + r^4}}{1+r^2+\sqrt{1+2r^2\cos 2\delta + r^4}}} \tag{9}$$

where $r = \sqrt{I_y/I_z}$ and $\delta = \varphi_y - \varphi_z$. The range of the ellipticity is $0 \le \varepsilon \le 1$. The linear, elliptical, and circular polarization correspond to $\varepsilon = 0$, $0 < \varepsilon < 1$, and $\varepsilon = 1$ respectively. If δ is 0 or π, the HHG will be linearly polarized. For other values of δ between 0 and π, the HHG will be elliptically polarized. In order to attain high ellipticity, the phase difference must be around $\pi/2$.

3. Result and discussion

We study the ellipticity of HHG from oriented polar CO molecules driven by a linearly polarized laser.A 30-fs 800-nm driving pulse with an intensity of $2\times10^{14}\ W/cm^2$ is used in our simulation. The electric field of the laser pulse is expressed as

$$\vec{E}(t) = E_0\cos(\omega t)sin^2(\frac{\pi t}{T})\vec{z}, \tag{10}$$

where E_0 is the amplitude of the driving field. Figure. 2(a)presents the ellipticity of the harmonic emission at two orientation angles 30° (red line) and 45° (black line). One can see that for the two orientation angles, strongly elliptically polarized harmonics are observed in a wide spectral range covering the plateau to the cutoff. In Fig. 2(b), the phase difference (blue line) and the ellipticity (black line) of the recombination dipole moment [13, 30] for CO oriented at 45° are also presented. Here the phase difference is shifted into $[-\pi, 0]$. Interestingly, the relative phase between the y, z components of the dipole moment is close to $-\pi/2$ for all the electronic momenta. As a result, the ellipticity of the dipole moment is quite large, as shown by the black curve. Furthermore, it is also shown that the ellipticity curve of the dipole moment in panel (b) is similar to that of the harmonics at the same orientation angle (black line) in panel (a). The electronic momentum is transformed into the harmonic order by the dispersion relation

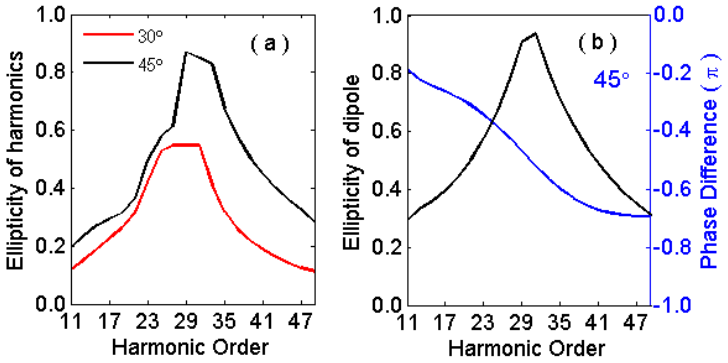

Fig. 2. (Color online) (a) The ellipticity of harmonics generated from CO for the orientation angle at 30° (the red line) and 45° (the black line). The horizontal axis represents the harmonic order. (b) The ellipticity (the black line) and phase difference (the blue line) of the recombination dipole moment for the orientation angle at 45°. The phase difference is shifted into $[-\pi, 0]$. The electronic momentum is transformed into the harmonic order.

$q\hbar\omega = E_p + I_p$, wherein E_p is the kinetic energy of the free electron with the momentum p. This phenomenon will be discussed latter.

The ellipticity of the harmonics for CO oriented at other angles from 0° to 90° is also studied. The map of the harmonic ellipticity is shown in Fig. 3(a) versus the harmonic order and the orientation angle. As shown in Fig. 3(a), strongly elliptically polarized harmonics are also obtained at other orientation angles ranging from 30° to 80°. In Fig. 3(b), the ellipticity of the dipole moment as a function of the orientation angle and the electronic momentum is presented as well. Here the electronic momentum is transformed into the harmonic order using the same dispersion relation. One can see that the phenomenon observed in Fig. 2 is not specific to the case when the molecule is oriented at angle 45°. As shown in Fig. 3, the ellipticity map of the harmonics in panel (a) also exhibits a quite similar shape to that of the dipole moment in panel (b). To explain this phenomenon, a theoretical analysis is performed based on the three-step model [24, 31] for high harmonic generation from oriented molecules. In this model, an electron first tunnels from the ground state, then oscillates in the field, finally recombines with the parent ion. The recombination step leads to the emission of a high-energy photon with two polarization components, parallel (z) and perpendicular (y) to the laser polarization. Since the first two steps are identical for the y, z components of the harmonics, the phase difference and amplitude ratio between the two components of the harmonics is mainly contributed by those of the recombination dipole moment $\vec{d}^*(p)$. Hence the ellipticity curves between harmonics and the recombination dipole moment exhibit a similar shape at the same orientation angle, as shown in Fig. 2 and Fig. 3. In other words, the recombination dipole moment $\vec{d}^*(p)$ is responsible for the large ellipticity of the harmonics over a wide spectral range for CO.

From the formula $\vec{d}^*(p;\theta) = \langle \exp(ipz)|\vec{r}|\psi_0(r;\theta)\rangle$ for the recombination dipole moment, one can see that the phase difference $\arg(d_y^*) - \arg(d_z^*)$ and the amplitude ratio $|d_y^*/d_z^*|$ of the recombination dipole moment are directly related to the spatial structure of the HOMO. In the following, we analyze the influence of the HOMO structure on the phase difference of $\vec{d}^*(p)$ in detail to grasp a deeper insight into the large ellipticity of the harmonics generated from the polar CO molecules. For comparison, we also discuss the case of non-polar N_2 molecule, which has a symmetric HOMO with a similar geometry (σ_g) to that of CO. Sectional views of

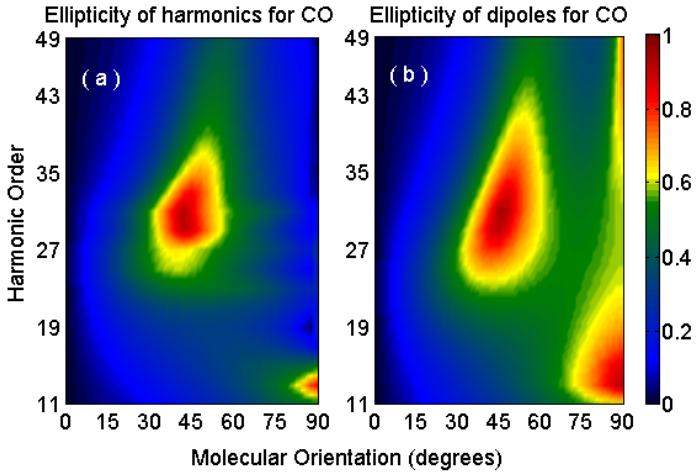

Fig. 3. (Color online) (a) The ellipticity of harmonics as a function of the orientation angle and the harmonic order. (b)The ellipticity of the recombination dipole moments versus the orientation angle and the electronic momentum which is transformed into the harmonic order using the dispersion relation $q\hbar\omega = E_p + I_p$. E_p is the kinetic energy of the free electron with the momentum p, Ip is the ionization energy of the target. For the two panels, the target is the polar CO molecule, the orientation angle and the harmonic order correspond to the horizontal and vertical axes respectively.

the HOMO for N_2 and CO at the orientation angle 45° are presented in Fig. 4. As shown in this figure, the section of the non-polar N_2 molecule in panel (a) exhibits a centro-symmetric structure. Then the wavefunction satisfies $\psi_0(x,y,z;\theta) = \psi_0(x,-y,-z;\theta)$ (for arbitrary value of x). However, for the nonsymmetric HOMO of CO this condition is not satisfied, as shown in panel (b). With Eq.(6), one can obtain $Re[d_j^*] = 0$ and $Im[d_j^*] \neq 0$ for N_2, $Re[d_j^*] \neq 0$ and $Im[d_j^*] \neq 0$ $(j = y,z)$ for CO, respectively. As a result the phase difference of $\vec{d}^*(p)$ for N_2 is either 0 or $\pm\pi$, as shown by the blue curve in Fig. 5(b). Whereas for CO, they can take other values including $\pm\pi/2$ for all the electronic momenta, as demonstrated in Fig. 2(b). The phase difference of the harmonics is dominated by that of the recombination dipole moment, as illustrated above. Therefore large ellipticity of the harmonics is obtained in a wide spectral spectrum, as presented in Fig. 2(a) by the black curve. Finally, it can be concluded from the above discussion that the nonsymmetric structure of the HOMO is the major origin of the ellipticity observed in the case of the oriented polar CO molecules.

Figure 5(a) shows the ellipticity of the harmonics generated from N_2 at the same orientation angles with Fig. 2(a). In contrast to CO, the nonzero ellipticity of the harmonics are only obtained in the vicinity of the structure minima in the HHG spectra, where the positions of the minima coincide with those in [30]. This nonzero ellipticity of the harmonics is well explained by the two-center interference effects, which is analogous to [16, 20, 21] for non-polar molecules. Comparison between the cases of CO and N_2 also shows that the ellipticity of the harmonics of CO is larger than that of N_2 for most of the orientation angles, as demonstrated in Fig. 2 and Fig. 5 for the orientation angles at 30° and 45°. Therefore our results suggest a potential application of HHG from polar CO molecules in generating the broadband large-ellipticity harmonics, which will benefit the application of HHG as a tool of detection in biology and materials science in the future.

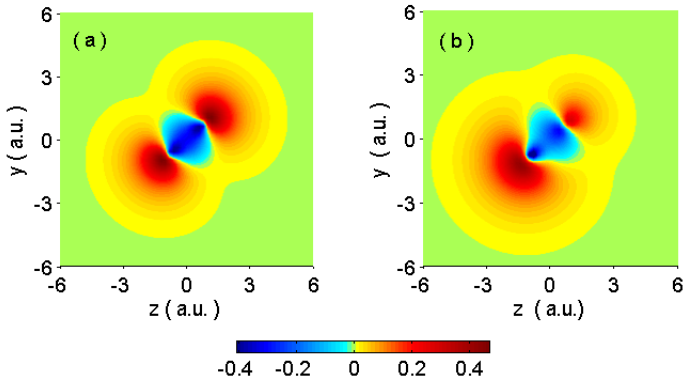

Fig. 4. (Color online) A view of the section parallel to the yz plane for N_2 in the left panel and CO in the right panel. The two target molecules are oriented at 45°.

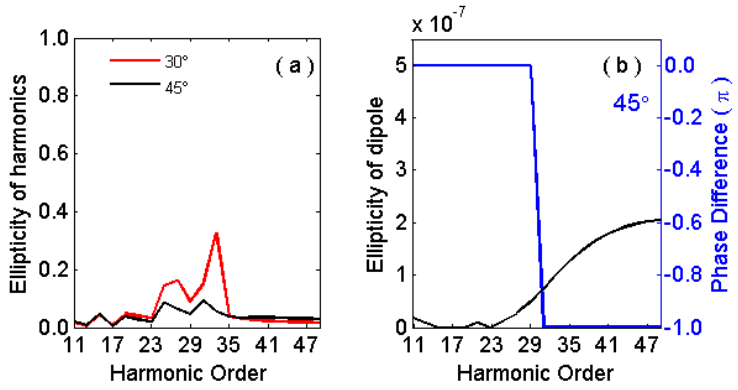

Fig. 5. (Color online) (a) The ellipticity of harmonics generated from the oriented N_2 at 30° (the red line) and 45° (the black line). The horizontal axis is the harmonic order. (b) The ellipticity (the black line) and phase difference (the blue line) of the recombination dipole moment for N_2 oriented at 45°. The phase difference is shifted into $[-\pi, 0]$. The electronic momentum is transformed into the harmonic order.

4. Conclusion

We use the example of CO to investigate the polarization characteristics of HHG from the oriented polar molecules driven by a linearly polarized laser. It is found that the harmonics over a wide spectral range are strongly elliptically polarized for the orientation angles ranging from 30° to 80°. The spectral range of large-ellipticity harmonics is covered from the plateau to the cutoff, while for non-polar molecules the harmonics only in the vicinity of the interference minimum are elliptically polarized. Further analyses show that the nonsymmetric structure of the HOMO is the major origin of the ellipticity of the harmonics observed in oriented CO molecules. Since the nonsymmetric structure is a general characteristic of the HOMO for polar molecules, the conclusions made from the results of CO can be extended to other polar molecules. Thus our investigations provide a method for generation of large-ellipticity XUV

pulses, which will benefit the application of HHG as a tool of detection in materials and biology science.

Acknowledgment

This work was supported by the National Natural Science Foundation of China under Grants No. 60925021, 10904045, 10734080 and the National Basic Research Program of China under Grant No. 2011CB808103. This work was partially supported by the State Key Laboratory of Precision Spectroscopy of East China Normal University.